Orhan Demir and Rauf Hurman Eric*

Rate and Mechanism of Reduction-Dissolution of Chromite in Liquid Slags

Abstract: The dissolution of chromite from the Bushveld Complex of South Africa in liquid slags was studied in the temperature range 1550° to 1665°C under argon gas. The slag compositions were similar to those of ferrochromium production and stainless steel making. Empirical relations between the slag composition and the dissolution of chromite were established through the use of a statistical model. The dissolution process was investigated by using the rotating cylinder technique and measured by the chemical analysis of the samples taken from the melt and the SEM-EDAX analysis of the reacted chromite cylinder samples. The chromite grains were depleted in iron and chromium as the dissolution progressed, leaving behind an alumina and magnesia rich spinel. The experimental data was evaluated by using kinetic models and mass transfer coefficients of chromium, iron and oxygen ions through the phase boundary between the solid chromite cylinder and the liquid slag were determined.

The dissolution of chromite in liquid slags increases with increasing stirring rate. SEM-EDAX studies on the reacted chromite cylinders showed that coring took place within the chromite grains subjected to dissolution for sufficient length of time. Chromium and iron concentrations in the chromite were decreasing from the centre towards the surface of the grains while aluminum and magnesium contents were increasing at the edges compared to the centre of the chromite grains. Furthermore, the slag rich in alumina and magnesia diffuses in bulk into the chromite with a net result of increase in the concentration of these elements.

The rate of dissolution of chromite in liquid slags was found to be controlled by the mass transfer of oxygen ions (O^{2-}) through the liquid phase boundary between the solid chromite and the liquid slag. The activation energy for the mass transfer of O^{2-} ions was calculated as 30.61 kCal/mol (128.07 kJ/mol).

Keywords: rate, mechanism, chromite, dissolution, slag

***Corresponding author: Rauf Hurman Eric:** School of Chemical and Metallurgical Engineering, University of the Witwatersrand, Johannesburg, South Africa. E-mail: Rauf.Eric@wits.ac.za
Orhan Demir: Tenova-Pyromet, Johannesburg, South Africa

1 Introduction

Ferrochromium is currently produced predominantly by the smelting of chromite ore in submerged-arc electric furnaces. The economics of the process largely depend on the grade and melting behavior of the ore and the slag properties.

Previous studies [1–6] indicate that the chromium in the discard slags is mainly in the form un-dissolved chrome ore and metal droplets. In plants that experienced high chromium losses (more than 11 percent) it was found that more than 60 percent of the chromium in the slag was in the form of un-dissolved or partly altered chromite particles. On a South African submerged-arc furnace, Van Der Colf [7] determined that the chromium recovery averaged 73.2 percent, chromium losses being 17.2 percent as oxide, 2.17 percent as metallic inclusions and 7.43 percent as dust and other losses.

Information on the dissolution behavior of chromite ore in liquid slags is necessary in minimizing the Cr losses to slag leading towards a more economically feasible process, or even towards making possible the use of the low grade chrome ores to produce a saleable ferrochrome metal. Although the kinetics of the chromite ore and solid Cr_2O_3 reduction has been investigated extensively in the past, the number of studies with chromite in molten slags is limited. Therefore, this work is believed to make an important contribution in understanding the dissolution behavior of chromite in a wide range of slag compositions at temperatures representative that of high carbon ferrochrome production and stainless steel making.

2 Experimental procedure

The empirical relations between the slag chemistry and the chromite dissolution under reducing conditions at 1600°C were established at a fixed rotational speed of 100 rpm. The effect of different levels of reducing conditions were tested by using graphite and molybdenum crucibles under a flow of argon gas, and the slag

temperature was 1600°C. Because of the large number of slag components and their comparatively large range, the experimental work was based on a statistical model. Statistical designing of experiments has the advantages that the experiments become more efficient and economical and the individual and the joint effects of different factors on the response can be evaluated together. A total number of 20 different slag compositions were used to define the response surface, i.e. chromite dissolution. On the other hand in the experiments to determine the rate and mechanism of the dissolution, the rotational speed changed from 60 to 800 rpm and the slag composition was initially fixed at 43% SiO_2, 21%Al_2O_3, 23% MgO and 13% CaO and the temperature varied from 1550° to 1665°C.

The data generated for chromite dissolution as a function of slag composition was fitted in a quadratic equation of the following type according to the statistical model:

$$Y(X) = \beta_0 + \sum_{i=1}^{4} \beta_i X_i + \sum_{i=1}^{4} \beta_{ii} X_i^2 + \sum_{i=1}^{4} \sum_{i<j} \beta_{ij} X_i X_j \qquad (1)$$

where Y = response ('percent dissolution'), β_0 = intercept, β_{ij} = parameter for X_i, X_i = mass percent ($X_1 = SiO_2$, $X_2 = Al_2O_3$, $X_3 = MgO$, $X_4 = CaO$).

The experimental method consisted of submerging a rotating chromite cylinder in a liquid slag melt, of appropriate composition, held in a graphite or molybdenum crucible. Approximately 350 g of slag was charged in the crucible to allow sufficient volume for the total immersion of chromite cylinders. The dissolution was measured by the chemical analysis of the samples obtained from the slag melt at predetermined time intervals.

The chromite cylinders were prepared from tabled and pulverized LG-6 chromite ore from the Bushveld Complex of South Africa. The chemical analysis of the ore is given in Table 1. By using the number of moles of cations per 32 moles of oxygen, the chemical formula of the sintered chromite was calculated to be [8]:

$$(Mg^{2+}_{4.38}, Fe^{2+}_{3.63})[Cr^{3+}_{10.7}, Fe^{3+}_{1.26}, Al^{3+}_{3.87}, Ti^{4+}_{0.085}, Fe^{2+}_{0.085}]O^{2-}_{32}$$

where round and square brackets represent tetrahedral and octahedral sites respectively. The method of calculation is given elsewhere [9].

Pulverized chrome ore with no binders was pressed in a steel mould under a uniaxial pressure of 6 tons to obtain fresh cylinders 15.6 mm in diameter and 17–19 mm in length. This was followed by sintering in the induction furnace under argon, at a flow rate of 2200 cm^3/min, at 1200°C for 2 hours. The density of the cylinders was 3.6 g/cm^3. Any cylinders having cracks after sintering, were rejected. Subsequent to sintering, the cylinders were drilled and attached to an alumina + stainless steel rod assembly by using alumina cement. The rod assembly attached to the chromite cylinder was rotated along its axis at a controlled speed determined by using a hand tachometer. The chromite cylinder could be raised or lowered by about 20 cm so that it could be removed or immersed into the melt. The gas-tight reaction chamber kept under a slightly positive pressure was continuously flushed by dried UHP argon gas at 2200 cm^3/min during the experiments. For the temperature measurements, a type B (Pt-6%Rh/Pt-30%Rh) thermocouple was used.

Master slags were prepared from chemically pure SiO_2, Al_2O_3, MgO, and CaO Powders mixed at appropriate proportions. The mixtures contained in a graphite crucible were melted in a high frequency induction furnace to provide homogenization and to increase the density of the samples. The molten slags were poured into a cast iron mould for solidification and solidified slags were then finally ground to powder form. The final slag compositions in the experiments were achieved by the addition of necessary amount of fresh powders to the master slags.

The reaction chamber heated by 50 kW, 3 kHz induction unit consists of a fused silica tube 500 mm long, with an external diameter of 120 mm and an internal diameter of 106 mm. The lower end of the tube is closed. The top

Chromite	Component, mass%							
	Fe_2O_3*	FeO	Cr_2O_3	Al_2O_3	SiO_2	TiO_2	MgO	CaO
As received	23.3	17.5	49.7	12.9	2.6	0.42	10.9	<0.2
Pulverized	24.2	18.2	49.7	12.8	2.8	0.42	10.7	0.19
Sintered	24.3	18.2	49.8	12.1	2.8	0.41	10.8	0.20

* Total Fe is calculated as Fe_2O_3

Table 1: Chemical analysis of the as received, pulverized and sintered chromite.

end is closed by a water-cooled brass plate, with an O-ring between the silica tube and the brass plate to ensure gas-tightness. A large graphite crucible fitting closely into the fused silica tube was used as the heating element. Depending on the desired level of reducing conditions in the chamber, graphite or molybdenum crucibles of 85×50 mm was placed in the graphite tube for melting. A graphite cover 2.5 cm thick was used as a radiation shield. The space between the heating element and silica tube at the periphery and at the bottom was packed by lampblack for insulation. This arrangement is shown in Figure 1.

As the chromite cylinder dissolves in the slag, SiO_2, Al_2O_3, MgO, CaO, total Fe, and total Cr contents of the slag change. The change in the total chromium content of the slag with time is taken as a basis in the measurement of the dissolution process. At a given time $\boldsymbol{t}$, during the dissolution of chromite in the liquid slag, the 'percent dissolution' is simply defined as the percentage of total chromium mass from the starting chromite cylinder released into the slag.

The chromium mass in the slag at a given period is determined by the chemical analysis of the slag samples. Thus, the 'percent dissolution' is given by the formula:

$$PercentDissolution \sim= \frac{(M)_{slag,t}(\%Cr)_{slag,t} + \sum_{i=1}^{n}(M)_{sample,i}(\%Cr)_{sample,i}}{0.3407(M)_{cylinder}} \quad (2)$$

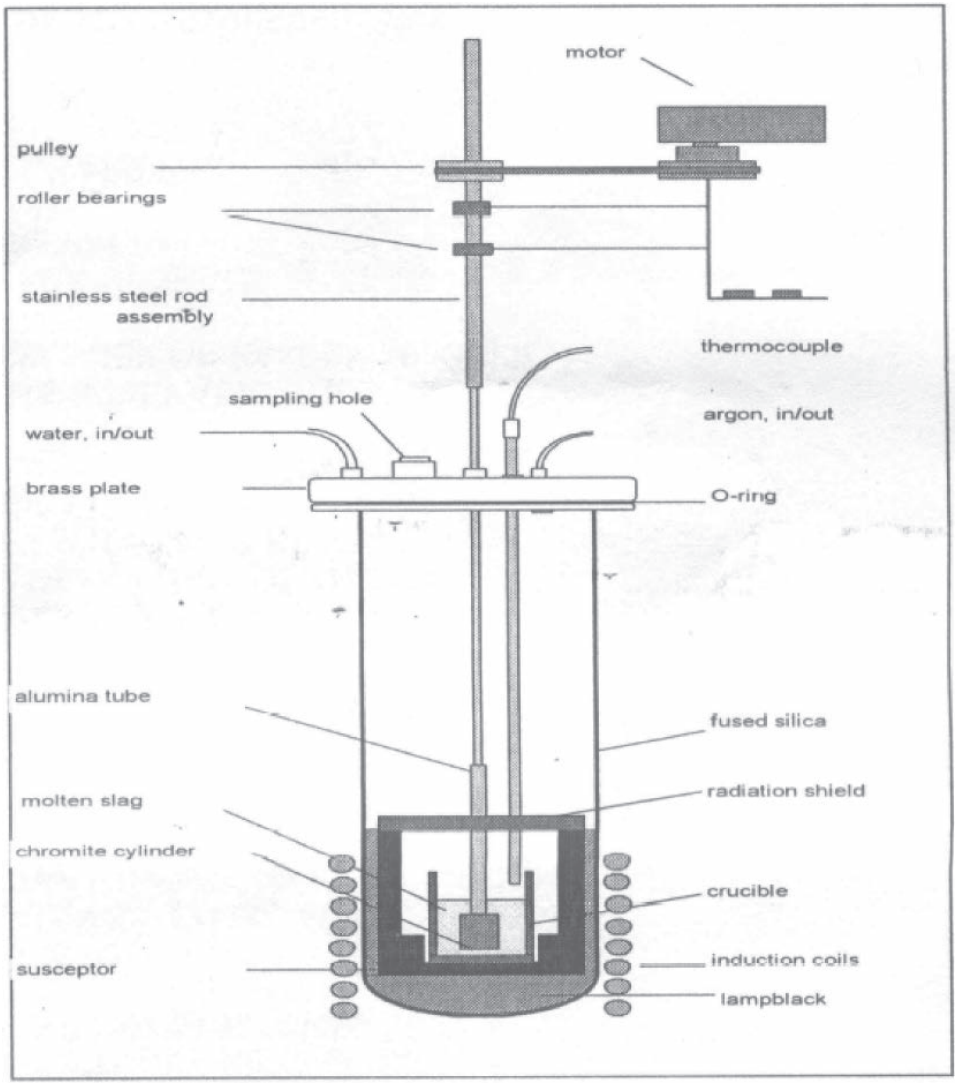

Fig. 1: Schematic representation of the reaction chamber. The arrangement of the graphite tube for electrical conduction, radiation shield, crucible containing the charge and the lampblack insulation.

where $(M)_{slag,t}$ is the slag mass (g), $(\%Cr)_{slag,t}$ is the percent chromium in the slag at time t, $(M)_{sample}$ is the sample mass (g), $(\%Cr)_{sample,i}$ is the percent chromium in a particular sample and $(M)_{cylinder}$ is the initial mass of the cylinder (g). There is 34.07 percent elemental chromium in the sintered chromite.

It was evident from the metallic formations rich in Cr, Fe and Si found in the solidified slag samples and on the crucible walls after the experiments that a certain amount of reduction took place. Therefore, equation 2 represents the dissolution and reduction behavior of chromite in liquid slags.

The slag was sampled at 3, 6, 12, 15, 20, 30, 45, 60 and 75 minutes after the rotation of the cylinder was started. A sample was withdrawn from the slag just before the immersion and start of the rotation to establish the initial composition. As and when necessary, slag samples were withdrawn at other times than those mentioned above.

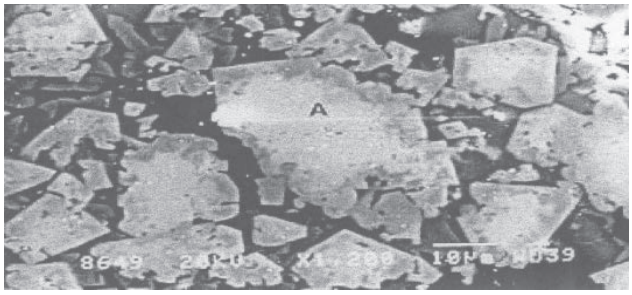

Fig. 2(a): Secondary electron image of the grains at the centre of a cylinder rotated at 104 rpm reacted for 4 minutes in the liquid slag of 43 SiO_2, 21 Al_2O_3, 23 MgO and 13 CaO contained in a graphite crucible at 1550°C, under argon. Dark areas are the slag phase and gray areas are the chromite phase. The average of the compositions of the chromite and the slag phase determined at various points given below.

	Ca	Mg	Al	Si	Ti	Cr	Fe
Chromite	5.50	11.03	8.89	5.41	0.18	23.33	7.84
Slag	8.86	9.65	8.89	17.83	0.78	3.59	8.24

3 Results and discussion

The results on the effect of slag composition on the chromite dissolution are too extensive and complex and have been given elsewhere [10] earlier and hence will not be repeated here. It would be a simple matter of calculation through the use of Equation 1 to see the effects of slag constituents and/or oxide ratios such as basicity on the dissolution behavior. However, very briefly, it can be mentioned that the chromite dissolution in slags in the SiO_2-Al_2O_3-MgO-CaO system increases with increasing alumina and increasing basicity of the slag. The three most important parameters playing the most dominant role in the dissolution of chromite in the order of importance are Al_2O_3 concentration, basicity and MgO/CaO ratio. The effect of increasing MgO content of the slag on the dissolution is positive when this increase is compensated by a decrease in CaO. However, when this increase in the MgO is provided by a decrease in Al_2O_3 content of the slag, the effect becomes negative.

During the experiments it was observed that the dissolution rate of chromite in liquid slag especially at higher rotational speeds was very fast suggesting that the process was not controlled by the solid state diffusion of any species in the solid spinel. The partially reacted chromite cylinders (for periods from 1 to 6 minutes) were examined in detail by the SEM-EDAX facility. Concentration profiles for chromium, iron, magnesium, aluminum and silicon were constructed along a line in a chosen grain. The SEM images and concentration profiles revealed zoning in the grains with an outer layer depleted in iron and chromium

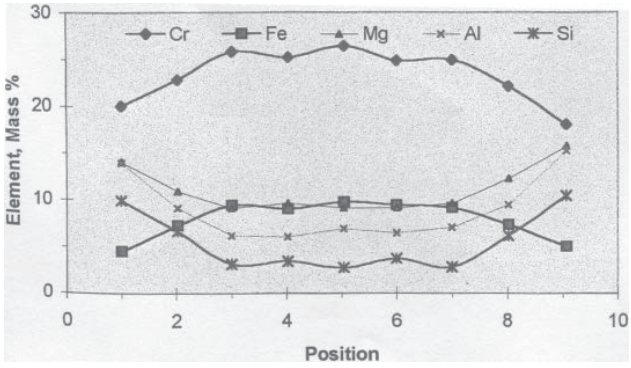

Fig. 2(b): Variations in element concentrations across grain (A) shown in Fig. 2(a)

and relatively enriched in magnesium and aluminum and an inner core which was identical to original unreacted chromite. It was also observed that the slopes of the concentration profiles became steeper with increasing immersion time. A typical plot is shown in Figure 2. The unaltered chromite spinel core indicated that any ion exchange between the chromite and the liquid slag took place only at the surface of the grains. Due to the fast dissolution, the chromite/slag phase boundary moves rapidly in a concentric fashion resulting in a growing slag volume in between the grains and exposing fresh chromite surface for further dissolution. The dissociation of oxides produces metallic cations and oxygen anions which dissolve in the slag.

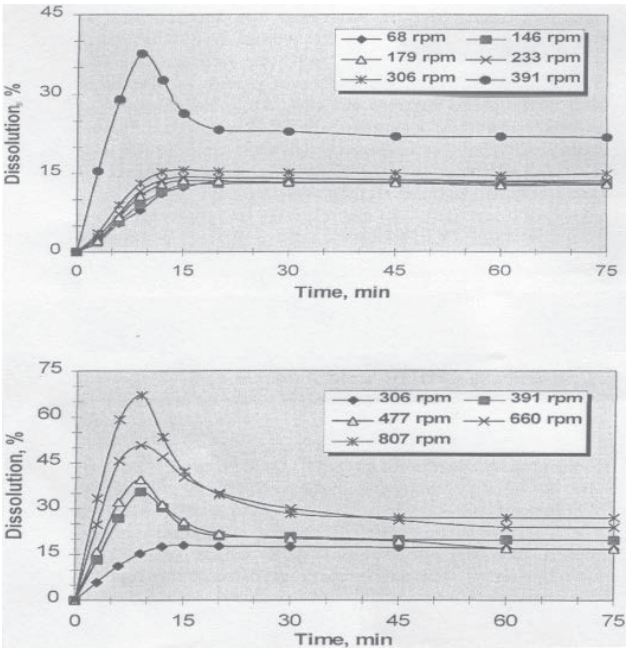

Fig. 3: Percent chromite dissolution versus time curves obtained for the dissolution of chromite in slags with 43 SiO_2, 21 Al_2O_3, 23 MgO and 13 CaO contained in graphite crucibles at 1550°C under argon, with the rotational speeds in the range of 68 to 807 rpm.

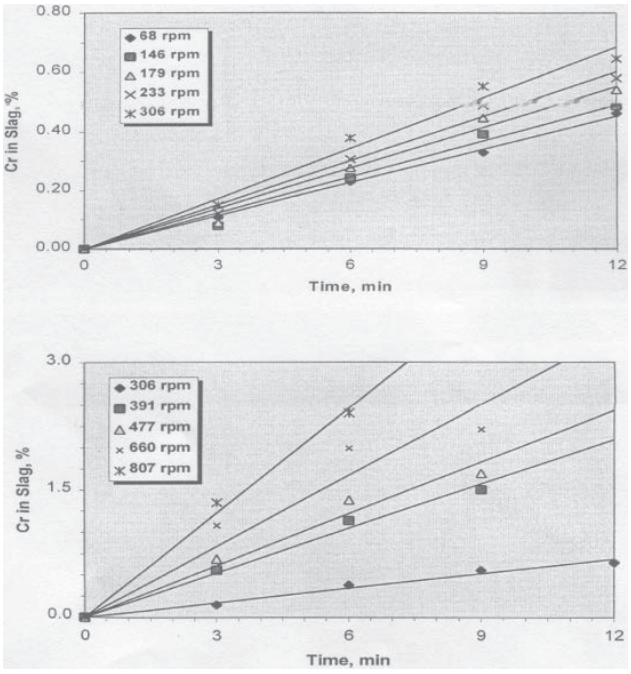

Fig. 4: Cr concentration in slags (mass percent) against time to obtain the specific rate constants for Cr (percent Cr in slag. min^{-1}) for rotational speeds of 68, 146, 179, 233, 306, 391, 477, 660 and 807 rpm.

3.1 Mechanism of chromite dissolution in liquid slag

The percent dissolution of chromite, calculated by equation 2, versus time curves obtained is illustrated in Figure 3. At relatively low rotational speeds from 68 to 306 rpm percent dissolution values showed limited increase.

Thereafter, at higher speeds, the dissolution values increased rapidly with the rotational speeds from less than 20% at 306 rpm to a maximum above 70% dissolution at 807 rpm. The plots of total Cr and Fe content of the slags (mass per cent) as a function of time produced straight lines with high correlation coefficients at all levels of stirring as shown in Figure 4.

The rate constants for Cr and Fe derived from the slopes of these lines as a function of rotational speed are given in Table 2. The Cr and Fe concentration in slags were back calculated from percent dissolution values to include the Cr and Fe contained in the samples withdrawn from the melt. It should be noted that the rate constants for speeds of 68 to 306 rpm were calculated for the first 12 minutes, for speeds from 391 to 660 rpm for the first 9 minutes and at 807 rpm for the first 6 minutes. This is due to the fact that dissolution is completed within these periods.

rpm	Rate constant (percent. min^{-1})		Corr. coefficient (r^2)	
	k_{Fe}	k_{Cr}	For k_{Fe}	For k_{Cr}
68	0.0243	0.0378	0.88	0.99
146	0.0253	0.041	0.83	0.98
179	0.0375	0.046	0.89	0.98
233	0.0389	0.050	0.97	0.98
306	0.0488	0.057	0.99	0.98
391	0.0742	0.174	0.87	0.99
477	0.0972	0.203	0.93	0.97
660	0.1067	0.278	0.88	0.92
807	0.2529	0.410	0.90	0.99

Table 2: Specific rate constants (percent. min^{-1}) for Fe and Cr passing from the chromite cylinder into the liquid slag (43 SiO_2, 23 MgO, 21 Al_2O_3, and 13 CaO) contained in graphite crucibles at 1550°C, under argon, at the rotational speeds in the range 68 to 807 rpm.

Moreover, as can be seen from Figure 3, the percent dissolution versus time curves for each rotational speed rise within these periods indicating that the chromium is being supplied into the melt. After these periods the curves start to decline due to reduction of dissolved chromium oxide by carbon at the crucible walls. The

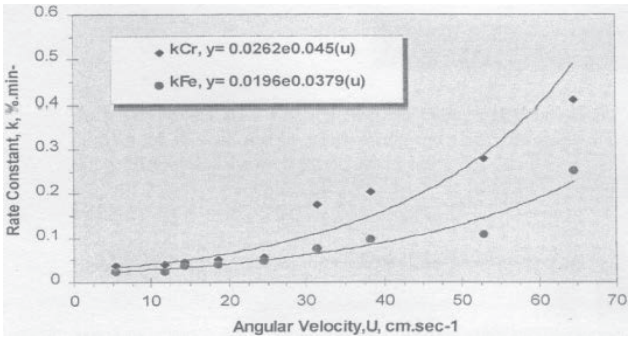

Fig. 5: Rate constants, (percent. min^{-1}), obtained for chromium and iron in the liquid slag as a function of the angular velocity, cm/sec of the chromite cylinder rotated at 68 to 807 rpm, 1550°C, under argon. Initial slag composition: 43 SiO_2, 21 Al_2O_3, 23 MgO and 13 CaO (R^2 for Fe = 0.96, for Cr = 0.92).

relationship between the angular velocity U (cm/s) of the chromite cylinder and the rate constants is shown in Figure 5. It is clear that the rate constant increases exponentially with velocity clearly suggesting the dissolution process is controlled by the mass transport (diffusion) of a species through the liquid boundary.

The dissolution of Chromite in this system consists of the following steps:

1. Dissociation of chromite at the chromite/slag phase boundary into constituent oxides such as FeO, MgO
2. Dissociation of oxides into their ions, i.e.,
   $Cr_2O_3 = 2Cr^{3+} + 3O^{2-}$
   $Fe_2O_3 = 2Fe^{3+} + 3O^{2-}$
   $Al_2O_3 = 2Al^{3+} + 3O^{2-}$
   $MgO = Mg^{2+} + O^{2-}$
   $FeO = Fe^{2+} + O^{2-}$
3. Reduction of Cr^{3+} and Fe^{3+} into their divalent state (due to the fact that in silicate slags under highly reducing conditions trivalent chromium and iron ions do not exist in significant quantities:
   $Cr^{3+} + e^- = Cr^{2+}$
   $Fe^{3+} + e^- = Fe^{2+}$
   $2O^{2-} = O_2 + 2e^-$
   Electrons being supplied by the free oxygen anions of the slag at the slag/graphite interface. This would than involve the reaction with the carbon of the graphite crucible walls and form CO gas bubbles which would be transported to the surface of the melt:
   $2C + O_2 = 2CO$.
4. Transport of chromium, iron, oxygen, aluminum, magnesium ions and electrons (electrons in opposite direction to ions) from the oxide/slag phase boundary to the bulk liquid slag.
5. Bulk transport of liquid slag into the enlarged grain boundaries, cracks and pores due to the hydrostatic pressure, surface tension effects and shear forces acting on the rotating cylinder.
6. Formation of a "new" slag phase in the vicinity of the chromite cylinder richer in the oxides of the spinel by the continuous dissolution of chromite. At this stage, the chromite cylinder is in the form of a solid-liquid mixture.

The dissolved species near the chromite cylinder then diffuse through the bulk liquid slag to the crucible wall where reduction of chromium and iron cations into metallic state takes place and a metal skin rich in chromium, iron and carbon forms.

Steps 1 and 2 cannot be rate limiting because of the high temperature involved where dissociation reactions involving oxides are fast. Similarly the reactions of step 3 can be considered very fast at high temperatures eliminating these as rate limiting. The SEM-EDAX investigations on the chromite cylinder reacted for a period of 1 minute at 104 rpm showed that the slag penetrated into the cylinder in less than 1 minute. The composition of this slag was representative of a mixture of the spinel phase and the initial slag composition. It can thus be assumed safely that steps 5 and 6 cannot be rate limiting. Therefore the analysis of the data will be confined to step 4, the diffusion of ions. However, the transport of electrons is a very fast process, and the concentration of aluminum and magnesium ions in the slag is relatively high. It can thus be assumed that no significant concentration gradients exist for aluminum and magnesium ions and accordingly the diffusion of these cations and electrons cannot be rate limiting. The liquid state mass transport of chromium, iron and oxygen ions from the chromite liquid phase boundary to the liquid slag are the remaining possible rate limiting steps.

3.2 Liquid state mass transport of chromium, iron and oxygen ions

At rotational speeds above 306 rpm the dissolution rate was very fast and maximum dissolution was attained within the first 6 to 12 minutes. The decrease in the cylinder diameter because of the dissolution causes the reactive surface area; A_s, the peripheral velocity; U, and the Reynolds number; R_e to decrease rapidly. In all experiments where 70% dissolution was achieved the cylinders were destroyed. At about 50% dissolution levels the chromite cylinders were distorted to a conical shape with a

length of about 15 mm and top diameter of 10 mm. Due to these facts, the reactive surface area; A_s was assumed to decrease linearly with dissolution and became zero at 70% dissolution. The calculation of A_s, and melt volume; V_m are given elsewhere [9] in detail.

Mass transport of chromium, iron and oxygen ions (each of which will be denoted as species; S) from the chromite cylinder through the phase boundary into the liquid slag in terms of A_s, V_m, mass transfer coefficients; k_S and the concentration gradient between the two phases is given by:

$$\frac{d(\%S_c)}{dt} = -k_S A_s \frac{(\%S_s - \%S_m)}{V_m} \quad (3)$$

where subscripts c, s and m refer to the chromite, slag/chromite phase boundary and the melt (liquid slag) respectively. The integral of Equation 3 is written as:

$$-(V_m/A_S)(\%s_S - \%s_m)\int_{S_{t=0}}^{S_{t=t}} d(\%S_c) = k_s \int_{t_0}^{t} dt \quad (4)$$

If the dissolution of any species is diffusion controlled, the plot of the left hand side of Equation 4, named as species transport; T_S against time should be a straight line slope of which would give the mass transfer coefficient of that species. Calculation of T_S for chromium (T_{Cr}), iron (T_{Fe}) and oxygen (T_O) are given in detail elsewhere [9] and their plots against time all produced straight lines with high correlation coefficients. Typical plots of species transport versus time are shown in Figure 6.

It should be noted here that Cr and Fe concentrations in the sintered chromite spinel is 34.07 and 17.01 mass percent (from Table 1). The total O^{2-} ion concentration in the starting chromite spinel, from Table 1, can be calculated as 29.2 mass percent. The O^{2-} concentration in the melt is determined by the chemical composition of the slag at each time interval through sampling. Considering the relatively small mass of chromite cylinder in comparison to the slag mass, the change in silica, alumina, magnesium oxide and calcium oxide contents of the slag due to the dissolution of chromite can be regarded as negligible. It was thus assumed in the calculations that the change in the oxygen ion concentration of the chromite is caused only by the change in its Cr_2O_3 and FeO contents and that the concentration of other oxides is relatively constant. The validity of this assumption was tested by calculating the cylinder mass at different stages of the dissolution by two different methods. The cylinder mass calculated using the percent dissolution values were very close to the values obtained by calculating the cylinder mass from the amount

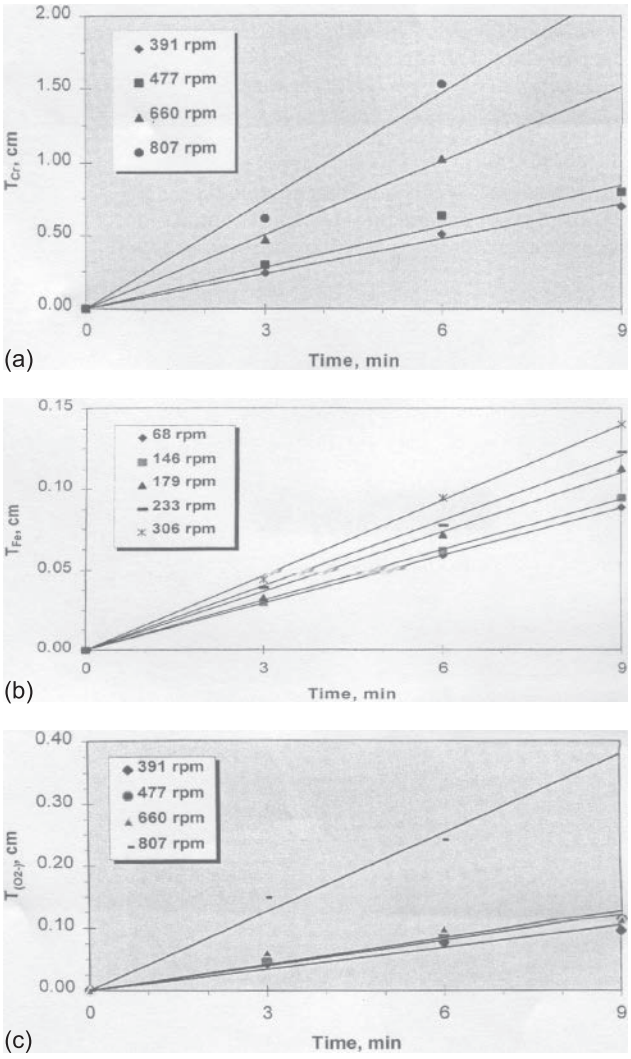

Fig. 6: The plots of (a) T_{Cr}, (b) T_{Fe}, (c) $T_{(O^{2-})}$ vs. time at various rotational speeds.

of oxides at a given time. The initial slag composition was the same for all experiments within analytical error limits, i.e., 43% SiO_2, 21% Al_2O_3, 23% MgO and 13% CaO.

The mass transfer coefficients obtained for chromium, iron and oxygen ions from the slopes of the plots of T_S versus time were re-plotted as a function of rotational speed as illustrated in Figure 7. In this figure the curve for O^{2-} lies below the curves for Cr and iron ions. Curves for Cr and Fe ions are very close to each other with Fe curve slightly under the Cr curve at rotational speed below 600 rpm. Above 600 rpm mass transfer coefficient of Fe becomes higher than the one for Cr. These findings strongly suggest that the oxygen ions are the slowest diffusing species followed by iron and chromium.

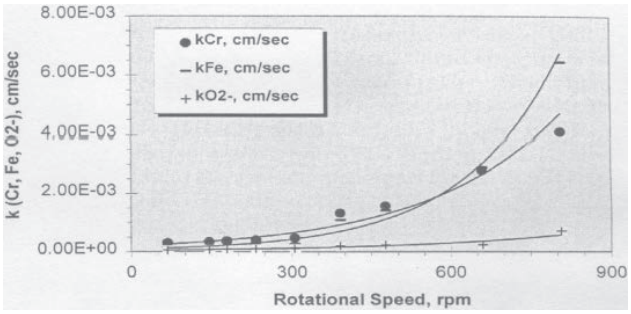

Fig. 7: Liquid state mass transfer coefficients of chromium, iron and oxygen as a function of rotational speed in the range 68 to 807 rpm.

3.3 Temperature dependence of mass transfer coefficients

The effect of temperature on the mass transfer coefficients was tested through a special series of experiments where the rotational speed of the cylinder was kept constant at 321 rpm. The slag and chromite cylinder were identical to the ones in the previous experiments and the same experimental procedure was employed, this time at three temperature levels; 1550°, 1585° and 1665°C. Again the species transport; T_S against time for the first 9 minutes of the dissolution were plotted from which mass transfer coefficients were derived. The logarithm of mass transfer coefficients of Cr, Fe and oxygen versus the reciprocal temperature were plotted as shown in Figure 8. The activation energies for the liquid state mass transport of Cr, Fe and oxygen ions were derived as 158.6 kJ/mol, 229.3 kJ/mol and 128.07 kJ/mol respectively from the slopes of the lines of Figure 8. There are no experimentally obtained activation energy values in the literature to be able to make comparisons. However, relating the mass transfer coefficients to angular velocity, viscous flow and diffusivity under the conditions of the rotating cylinder system through a mathematical analysis it is possible to calculate a range for activation energies of the three species in question from known values of angular velocity, kinematic viscosity and the experimentally derived mass transfer coefficients. The details of this procedure are given in detail elsewhere [9]. The activation energy ranges derived from the mathematical analysis are 103 to 176 kJ/mol for chromium, 112 to 200 kJ/mol for iron and 130 to 210 kJ/mol for oxygen. The experimentally derived values of this work mentioned above compare reasonably well with the range of values.

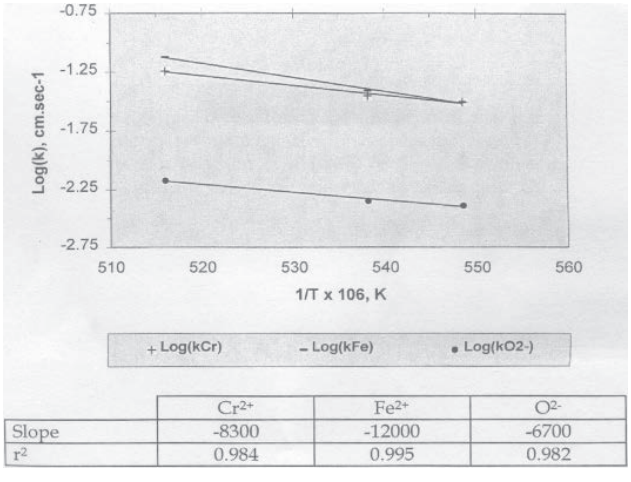

	Cr^{2+}	Fe^{2+}	O^{2-}
Slope	-8300	-12000	-6700
r^2	0.984	0.995	0.982

Fig. 8: Effect of temperature on the liquid state mass transfer coefficients of chromium, iron and oxygen at 321 rpm. (Slope = −0.4342E/R).

The mass transfer coefficient of a species during the dissolution of a solid in a liquid solvent is related to the diffusion coefficient of the species and the phase boundary thickness (δ) between the solid and the liquid phase by $k = D/\delta$. The thickness of the chromite/slag phase boundary decreases with an increase in the rotational speed of the chromite cylinder. The rate of decrease of the boundary layer is the same for chromium, iron and oxygen. Therefore, the differences in the mass transfer coefficients of chromium, iron and oxygen ions are caused by their diffusive abilities in the system, which is reflected by their diffusion coefficients. The mass transfer coefficients derived from experimental data for chromium, iron and oxygen ions in this study clearly supports the finding that the mass transport of oxygen anion controls the rate of the dissolution of chromite in the liquid slag of this study. Oxygen anion is thus the slowest diffusing species. This is not surprising as the size of the oxygen anion is much greater than that of the iron and chromium cations. The mass transfer coefficients for oxygen are an order of magnitude lower than the mass transfer coefficients of chromium and iron ions.

4 Conclusions

Results obtained from the experiments conducted by rotating chromite cylinders in liquid silicate slags showed that the dissolution of chromite increases with increasing rotational speeds. SEM-EDAX studies on the reacted chromite cylinders indicated that coring took place within the partially reacted chromite grains. Chromium and iron concentrations in the chromite phase were decreasing when moving from the centre toward the surface of the grains. Aluminum and magnesium contents, on the other hand, showed an increase at the edges compared to the central zones. Furthermore, the slag phase rich in alumina and

magnesia compared to the chromite spinel diffuses into chromite with a net result of increase in the concentration of these. At the last stages of the dissolution process the chromite was highly depleted in iron and chromium and was mainly consisting of magnesia, alumina and silica.

The mechanism for the dissolution of chromite was established on the basis of experimental observations and data. When the chromite cylinder is immersed in the slag, a new liquid slag phase forms between the solid chromite and the bulk liquid slag (forming the initial boundary layer), possibly with a composition close to that of the chromite spinel. The driving force for diffusion is the composition difference between the phase boundary and the liquid slag. Parallel to this, the liquid slag continuously penetrates into the grain boundaries, micro defects and pores in the solid chromite because of the hydrostatic pressure exerted by the liquid phase and the centrifugal forces acting on the system. This increases the surface area of the boundary layer between the solid and liquid phases. Dissolution proceeds by the diffusion of ions from the chromite phase into the liquid slag. The rate and extent of the chromite dissolution depends on the renewal of the boundary layer since the concentration of the diffusing species in the boundary layer can increase up to a certain extent (the equilibrium levels) after which they have to be washed away to leave space for further dissolution. The iron and chromium ions diffuse through the bulk slag to the graphite crucible wall where they are reduced to metallic state by carbon and produce CO gas. CO gas bubbles, after reaching a certain critical size, move through the bulk slag toward the surface and eventually join the gas phase.

By using well established kinetic models and using the dynamic principles of the rotating cylinder technique, the diffusion oxygen anions was found to be the most likely rate limiting step in the chromite dissolution. The mass transfer coefficients of the chromium, iron and oxygen ions as well as their activation energies were derived. The activation energy for the mass transfer of oxygen anion (O^{2-}) the diffusion of which is the rate limiting factor was found as 128.07 kJ/mol.

Acknowledgement: The authors are grateful to Ferroalloy Producers Association of South Africa for co-sponsoring this project.

Received: August 10, 2012. Accepted: November 16, 2012.

References

[1] E. J. Oosthuyzen and E. A. Viljoen, Quantitative mineralogy applied to a study of the process involved in the production of ferrochromium from Transvaal chromite ore, Proc. XIV Int. Mineral Processing Congress, Toronto, 1982, Canadian Inst. of Metallurgists, VIII, 6.1–6.17.

[2] D. I. Ossin, Liquidus temperature, viscosities and electrical conductivities of lime containing slags produced during the smelting of high carbon ferrochromium and ferrochromium silicide alloys, NIM Rep. No. 1366, Oct. 1971, Johannesburg, 15 p.

[3] T. R. Curr, A. Wedepohl and R. H. Eric, The dissolution of a Transvaal chromite in liquid silicate slags under neutral conditions between 1545°C and 1660°C, 3rd International Conference on Molten Slags and Fluxes, University of Strathclayde, U.K, June 1988, London Institute of Metals, 1989, pp. 298–304.

[4] O. Demir, Reduction of chromite in liquid Fe-Cr-Si alloys, M.Sc. thesis, 1992, University of the Witwatersrand, Johannesburg.

[5] S. Xu and W. Dai, The melting behavior of chromite ores and the formation of slags in the production of high carbon ferrochromium, INFACON 6, International Ferro Alloys Congress, Cape Town, 1992, Vol. 1, pp. 87–92.

[6] T. Enokido, H. Katayama, T. Kuwahara, F. Masaki and T. Sasaki, Influence of slag composition and reaction mechanism; Production of ferrochrome by smelting reduction in a stirred bath – II, iron making, the 107th ISIJ meeting, Tetsu-to-Hagane, Vol. 70 (4), 1984, pp. S117–124.

[7] R. C. Urquhart, The production of high carbon ferrochromium in a submerged arc furnace, Minerals Sci. Eng., Vol. 4, no. 4, October 1972, pp. 48–65.

[8] W. M. Donald and D. S. Ronald, Test Statistics for mixture models, Techno-metrics, Vol. 16, No. 4, November 1974, pp. 533–537.

[9] O. Demir, Dissolution of chromite in liquid Slags, Ph.D. thesis, 1999, School of Process and Materials Engineering, University of the Witwatersrand, Johannesburg, South Africa.

[10] O. Demir and R. H. Eric, Dissolution of chromite in slags, Proceedings of the Fray International Symposium on Metals and Materials Processing in a Clean Environment, 27 November–1 December 2011, Cancun, Mexico.